ALSYSTECH
Journal of Education Technology

e-ISSN : 2988-442X
p-ISSN : 2988-4403

Index : Dimensions, Scilit, Crossref, Garuda, Semantic, Google Scholar, Base, etc

https://doi.org/10.58578/alsystech.v2i2.3082

DAMPING FACTORS IN THE INTERPRETATION OF GEOELECTRIC DATA (CASE STUDY: MALALAK AGAM ROCK STRUCTURE)

Ayu Ashari Sembiring & Akmam
Universitas Negeri Padang
akmam_db@fmipa.unp.ac.id

Article Info:

Submitted:	Revised:	Accepted:	Published:
May 20, 2024	May 23, 2024	May 26, 2024	May 29, 2024

Abstract

This research aims to optimize the damping factor so that the results of Geoelectric data inversion are stable and in accordance with current geological conditions in Malalak Agam. This type of research is a descriptive research using secondary data in the form of pseudo-type resistance data and electrode spacing obtained from research in the field of Geoelectric exploration in the Department of Physics at Padang State University (UNP). This data is obtained from Geoelectric secondary data and location supporting data. The geoelectric data processing stage is carried out using Res2dinv software which is used to model in 2-D using least-square inversion. The results showed that based on the interpretation of the data, the suitable damping factors in Malalak Agam District, West Sumatra, were the initial damping factor (0.2 – 0.25) and the minimum damping factor (0.01 – 0.1) because on trajectory 2 At the third measurement point 160 meters from point 0 was dominated by limestone and

sandstone rocks. The existence of Limestone acts as a slip field, and there is Sandstone right above it which causes large-scale landslides from the first to fifth measurement points (315-160 meters from point 0) and on trajectory 3 at this time there is a landslide with a small volume, it is estimated that the avalanche is at the second measurement point 120 meters from point 0 with an avalanche thickness ranging from approximately 5 meters.

Keywords : Damping Factors, Geoelectric, Res2dinv, Inverse

INTRODUCTION

Geoelectric data interpretation is very important in natural resource exploration and geological mapping (Rolia & Sutjiningsih, 2018). Geoelectric resistivity data interpretation also depends on various other factors, such as the quality of the data obtained, the measurement techniques used, and the understanding of regional geology (Jamaluddin & Umar, 2018). Geoelectric data interpretation is used to understand the subsurface structure of the earth and estimate the potential of natural resources in a region (Sheishah dkk., 2022). The structure of the earth's subsurface can be interpreted using Geophysical methods, one of which is the resistivity Geoelectric method. Geoelectric resistivity is a Geophysical method used to study the electrical properties of the earth by measuring the electric field generated by electric currents flowing inside the earth and can model the structure of the earth's subsurface (Argobi, t.t.)

Geoelectric resistivity methods are divided into two types of modeling (Olubusola dkk., 2018). the first is forward modeling is the process of predicting or calculating data based on mathematical models by giving certain values to model parameters by conducting experiments (trial and error) to find compatibility between theoretical data and models. The second is inverse modelling, estimating the numerical value of the parameter model based on observation data using a certain model and matching the data (data fitting) to find model parameters that fit with the observation data(Gallardo & Meju, 2011).

Inversion modeling is a mathematical approach used in various fields of science and engineering to estimate model parameters from observational data by minimizing the difference between the data predicted by the model and the observed data. In inversion

modeling, model parameters are obtained directly from observed data, which is the opposite of forward modeling where model parameters are used to predict expected data. The inversion modeling process involves automatic modification of the model parameters to achieve a better fit between the model calculation data and the literative observational data until the model response matches the observational data (Gupta dkk., 1997).

Geoelectric data processing using the Resistivity method requires an acquisition process with the Least-square Inversion method. Least-square inversion aims to find Geoelectric parameters that fit with observational data (Lestari dkk., 2019). Inversions in Geoelectric data are carried out with the aim of obtaining models that describe the distribution of resistivity or subsurface conductivity more accurately. Geoelectricity is often used for natural resource exploration because it does not damage or interfere with the material being observed or tested. Geoelectric methods can provide good spatial resolution so that they can map subsurface structures in high enough detail. Interpretation of geoelectric data generally uses the inversion method (Mulia dkk., 2018).

Inversion methods for interpreting Geoelectric data can be done with relative ease. Estimation of rock types based on actual type resistance can be done well if there is a good knowledge of local geology(Okechukwu & Abanum, 2020). Each component in a rock layer has different electrical properties, and the determination of the amount of resistance of a rock type depends on a number of factors, including water content, porosity of rocks, solubility of salts in water and rocks, and temperature. Water-saturated rocks will have lower type resistance than dry rocks (Pimienta dkk., 2019).

The inversion process begins with the initial value or initialization of the model parameters which is an initial estimate of the distribution of parameters to be estimated (Permana dkk., 2020). This initial value is important because it can affect the convergence and quality of inversion solutions. When different initial values or different approaches are used in determining initialization, it can result in different solutions in the inversion process. To reduce the uniqueness of the inversion results, a damping factor is given in order to stabilize the inversion results (Melani dkk., 2021).

Damping factors are constraints used to reduce uncertainty in inversion results and produce a more stable solution. Inversion tends to produce models that "overfit" observational data. By applying damping factors can limit the complexity of the model generated during the inversion process by adding regulatory terms into objective functions

that will be minimized during the inversion process (Hansen, 2010). These objective functions typically try to minimize the error between the calculation data and the observation data. The optimal damping value should strike a good balance between reducing uncertainty and overfitting in the inversion solution. Damping factors that are too high can cause loss of detail and resolution in the resulting model which can reduce the model's ability to capture phenomena accurately. Too small a damping factor makes the inversion solution very sensitive to noise in the data, resulting in unstable model parameters if the observed data has a high noise level (Binley dkk., 2015).

METHODS

This type of research is a descriptive research using secondary data in the form of pseudo-type resistance data and electrode spacing obtained from research in the field of Geoelectric exploration in the Department of Physics at Padang State University (UNP). This study has two variables, namely independent variables and dependent variables. Independent variables are variables that are not influenced by other variables, while dependent variables are variables that are influenced by other variables. In this study, the independent variable is the type and depth resistance and the dependent variable is the accompanying factor. This data is obtained from Geoelectric secondary data and location supporting data. The geoelectric data processing stage is carried out using Res2dinv software which is used to model in 2-D using least-square inversion. Apparent resistivity is the resistivity that can be measured using the geoelectric method. The obvious resistivity value represents the distribution of medium resistivity values; however, apparent resistivity cannot be immediately read as the medium's resistivity value *(Sari, 2018)*. ϱ_α represents the apparent resistivity in Equation (1).

$$\varrho_\alpha = K\frac{V}{I} \qquad (1)$$

K is the configuration-type-dependent geometric factor; $\rho\alpha$ is the apparent resistivity value; V is the potential difference; and I is the electric current strength. Equation (1) yields the following K value:

$$K = 2\pi \left\{\left(\frac{1}{r_1} - \frac{1}{r_2}\right) - \left(\frac{1}{r_3} - \frac{1}{r_4}\right)\right\}^{-1} \qquad (2)$$

K is the electrode arrangement's geometric factor, and its value varies as the distances between the electrodes alter *(Rahmani dkk., 2020)*

In the Wenner-Schlumberger arrangement, two current and two potential electrodes placed in a straight line are employed as the four electrodes. The ratio of the distance between the AM and MN electrodes is observed to serve as the comparison factor "n" for the Wenner-Schlumberger arrangement. There is a constant spacing rule

scheme in this design. If the distance between the potential electrodes (MN) is a, then the distance between the current electrodes (A and B) is equal to 2na+a*(Pasa'Bi, 2021)*. The geometric factors of the Wenner-Schlumberger configuration in equation (3) are as follows:

$$k = n(n+)1\ \pi a \qquad (3)$$

Where a represents the separation between electrodes M and N.

The inversion modelling process automatically modifies model parameters to achieve a better match between model calculation data and observation data, which is carried out literally until the model response matches the observation data*(J., 2013)*. Initial estimates can be added to the model parameters in the inversion process with the following correction factors:

$$\Delta m = [G^T G + \varepsilon^2 \underline{W}]^{-1} G^T \Delta d \qquad (4)$$

The data difference vector is Δd, the correction parameter vector is Δm, the damping factor is ε, and G is the Jacobian matrix storing partial differential data against the model parameters (Akmam, 2018).

RESULTS

The parameter calculated in this research is apparent resistivity. The parameters interpreted are actual resistivity and depth.The estimated parameters are the results of rock structure analysis from the Wenner-Schlumberger configuration. Data collection was carried out using six passes. Trajectories 1, 2, 3, 4, 5 and 6 have the same path length, namely 315 meters with an electrode spacing of 5 meters.

The following results of data interpretation on the first pass can be seen in Figure 1.

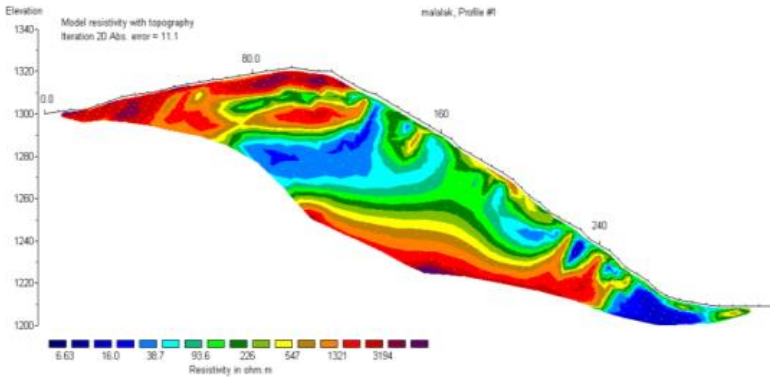

Fig 1. Distribution of resistivity and path depth 1

Based on Figure 1 stretches from coordinates (00'22.259 S, 100'17.300', height 1300 masl), which is the peak point and (00'25.488 S, 100'16.412', height 1209 masl), which is the lowest point (on the edge of the road).is the distribution of resistivity anomalies with an initial damping factor of 0.25 and a minimum damping factor of 0.01. The resistivity value is 6.63 Ωm – 3194 Ωm with an error percentage of 11.1%. Identify rock types, thickness and depth of subsurface layers along route one based on the highest point (at the top), namely 80 meters from point 0 (peak point), 120 meters from point 0, 160 meters from point 0, 200 meters from point 0 and 280 meters from zero.

At the first point, 80 meters from point 0, four rock layers were found: sand, clay, sand, and clay. At this point, it was identified that limestone and andesite rocks may occur at a depth of 1290–1297 meters above sea level with a thickness of 7 meters; the clay is at a depth of 1280–1289 meters above sea level with a thickness of 9 meters; andesite is at a depth of 1310-1320 meters above sea level with a thickness of 10 meters; and sandstone is at a depth of 1298–1309 meters above sea level with a thickness of 9 meters.

At the second point, 120 meters from point 0, four rock layers can be seen: sand, clay, and grit. Sandstone lies at a depth of 1305–1310.

The third point, 160 meters from point 0, found three layers of rock: black sand, black sand, and andesite. Black sand is at a depth of 1258–1290 meters above sea level with a thickness of 32 meters, black sand is at a depth of 1240–1257 meters above sea level with a depth of 18 meters, and andesite is at a depth of 1230–1240 meters above sea level with 10 meters thick.

Four rock layers were identified at the fourth point, 200 meters from point 0: andesite, sandstone, clay, and limestone. Andesite is at a depth of 1220–1224 meters above sea level with a depth of 4 meters; sandstone is at a depth of 1270–1275 meters and 1225–1237 meters above sea level with a depth of 10-12 meters; and clay is at a depth of 1245–1259 meters above sea level with a depth of 14 meters.

At the fifth point, 280 meters from point 0, one type of rock, clay, was identified. The clay is 1205-1230 meters above sea level and 25 meters thick, so it can cause landslides when it rains.

The results of data interpretation show that at the first measurement point, 80 meters from the zero point, it is dominated by very thick andesite rock with a layer of andesite covered by sandstone. At the second measurement point, 120 meters from the zero point, it is dominated by clay rock, sandstone and clay rock. At the fifth measurement point, 315 meters from point 0, it is dominated by clay rocks with a thickness of 25 meters. The risk of landslides can increase if there is thick enough clay. When thick clay is adjacent to limestone and andesite rock formations, the likelihood of landslides increases, especially if water pressure from the saturated clay interacts with harder rock. This can cause the weight of the soil to increase above the slip plane and cause unstable ground movement. A translational slip plane is one in which the movement of rock masses and soil is either sloping or level.

Following are the results of data interpretation on the second pass, which can be seen in Figure 2.

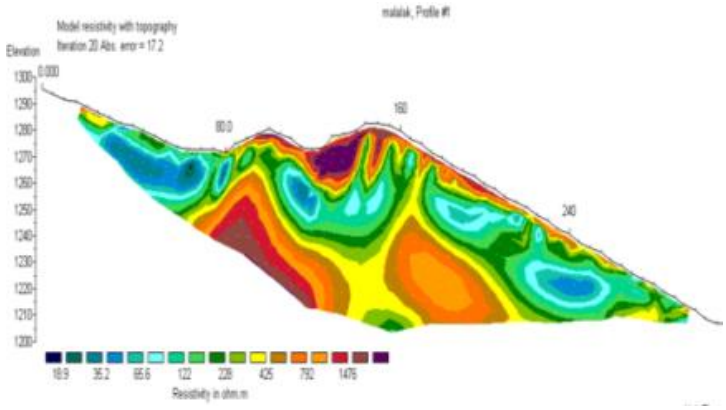

Fig 2. Distribution of resistivity and path depth 2

Based on Figure 2 stretches from coordinates (00'22.250 S, 100'17.214', height 1296 masl) to ith (00'22.385 S, 100'17.206', height 1207 masl. Field data collection carried out on track 2 has a track length of 315 meters with an electrode spacing of 5 meters. The distribution of resistivity anomalies with an initial damping factor of 0.2 and a minimum damping factor of 0.05. The resistivity value is 18.9 Ωm – 1476 Ωm with an error percentage of 17.2%. Identification of rock types, thickness and depth of subsurface layers along Track 2 was taken at several measurement points, namely 80 meters from point 0 (top point), 120 meters from point 0, 160 meters from point 0, 200 meters from point 0 and 280 meters from point zero.

At 80 meters from point 0, three rock layers were identified: andesite, sandstone, and clay. Andesite is at a depth of 1235–1244 meters above sea level and has a thickness of 9 meters, and sandstone is at a depth of 1245–1254 meters and has a thickness of 9 meters. The clay is at a depth of 1260–1270 meters and has a thickness of 25 meters.

At the second point, 120 meters from point 0, four types of rock were identified: black sand, clay, clay, and andesite. Black sand is at a depth of 1210-1239 meters above sea level and has a thickness of 29 meters; clay is at a depth of 1250-1259 meters above sea level and has a thickness of 9 meters, and andesite is at a depth of 1260-1270 meters above sea level and has a thickness of 9 meters.

At the third point, 160 meters from point 0, three rock layers were identified: limestone and sandstone. Limestone is at a depth of 1250-1269 meters and 1202-1206 meters above sea level with a thickness of 4-19 meters, while sandstone is at a depth of 1270-1280 meters and 1207-1249 meters above sea level with a thickness of 42 meters.

At the fourth point, 200 meters from point 0, three rock layers were identified: clay, clay, and sand. Clay is at a depth of 1230-1244 meters above sea level and has a thickness of 14 meters, sand at a depth of 1260-1265 meters, and 1205-1229 meters above sea level and has a thickness of 5-24 meters.

At the fifth point, 280 meters from point 0, it was identified that there were three types of rock layers: clay, sand and clay. The clay is at a depth of 1210-1229 meters above sea level with a thickness of 19 meters; the sand is at a depth of 1230-1244 meters and 1202-1209 meters above sea level with a thickness of 7-14 meters; and the sand is at a depth of 1245-1255 meters with a thickness of 10 meters.

The results of data interpretation show that at the first measurement point 80 meters from point 0 it is dominated by clay rock, sandstone and dolomite. At the third measurement point, 160 meters from point 0, it is dominated by limestone and sandstone. The presence of Limestone acts as a slip surface, and there is Sandstone right above it. The presence o*f dolomite beneath Sandstone rocks mixed with Clay can also affect slope stability. Differen*ces in physical and chemical properties between sandstone, dolomite and clay can cause cracks and greater ground movement and increase the risk of landslides. Currently there is a landslide with a large volume at the third measurement point 160 meters from point 0. The landslide material is soil mixed with sand and gravel. The type of slip plane is translational, where the movement of soil and rock masses on the slip plane is flat or sloping. The results of the interpretation of previous research show that there are layers that are the same as the rock layers obtained in previous research.

Following results of data interpretation on the third track can be seen in Figure 3.

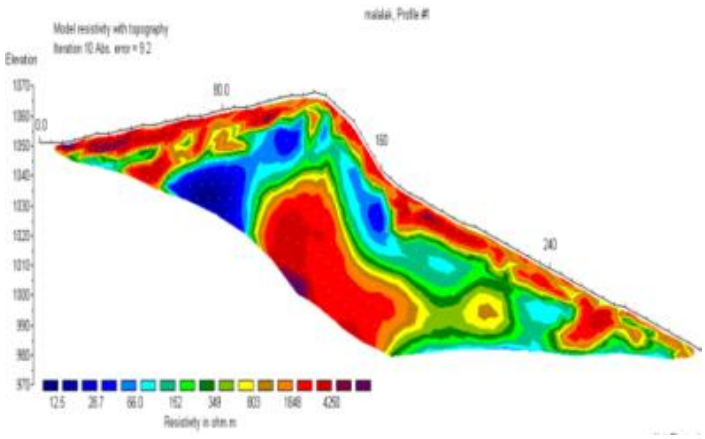

Fig 3. Distribution of resistivity and path depth 3

Based on Figure 3 stretches from coordinates (00'22.705 S, 100'16.318', altitude 1299 masl) to ith (00'25.488 S, 100'16.206', altitude 1182 masl). The distribution of resistivity anomalies with an initial damping factor of 0.05 and a minimum damping factor of 0.1. The resistivity value is 12.5 Ωm – 4250 Ωm with an error percentage of 9.2%.

Two rock layers, clay and sand, were identified 80 meters from point 0; the clay layer is at a depth of 1022–1039 meters above sea level and has a thickness of 17 meters, while

the sand layer is at a depth of 1040–1055 meters above sea level and has a thickness of 15 meters.

At the second point, 120 meters from point 0, three rock layers were identified: andesite, limestone, and sandstone. Andesite is at a depth of 1000–1029 meters above sea level and has a thickness of 29 meters; limestone is at a depth of 1040–1054 meters and has a thickness of 14 meters; and sandstone is at a depth of 1055–1065 meters and 1030–1039 meters and has a thickness of 9-10 meters.

At the third point, 160 meters from point 0, it was identified that there were four rock layers: andesite, limestone, clay, and sand. Andesite is at a depth of 985-1001 meters above sea level with a thickness of 9 meters, limestone is at a depth of 1010-1014 meters with a thickness of 4 meters, clay is at a depth of 1015-1039 meters with a thickness of 24 meters, and sand is at a depth of 1040- 1045 meters and 10 meters above sea level.

At the fourth point, 200 meters from point 0, three rock layers were identified: black sandstone, black sand, and andesite. Black sandstone is at a depth of 990-999 meters above sea level with a thickness of 9 meters, black sand is at a depth of 1000-1019 meters and 980-989 meters above sea level with a thickness of 9-19 meters, and andesite is at a depth of 1020 -1030 meters above sea level with a thickness of 10 meters.

The fifth point was identified 240 meters from point 0 and consists of three rock layers: lime, clay, and sand. Kimberlite is 9 meters thick at a depth of 980-989 meters above sea level, and clay is 19 meters thick at a depth of 990-1009 meters. The sandstone is 10 meters thick at 1010-1020 meters above sea level.

The results of data interpretation show that on this route there are several rock layers. At the first measurement point, 80 meters from point 0, it is dominated by dolomite, limestone and clay. At the third measurement point, 160 meters from point 0, it is dominated by dolomite, clay and limestone rocks. At this measurement point there is a slip area.

The presence of very thick clay creates conditions that are susceptible to soil movement. Limestone tends to be harder than clay, but can be a zone that is susceptible to deformation when stress or environmental changes occur. The presence of mechanically harder dolomite can strengthen slopes, but can also create the potential for landslides if there is friction between different rock layers. At the fifth measurement point, 240 meters from point 0, it is dominated by dolomite and clay. Currently a small volume landslide is

occurring on this track. It is estimated that the landslide will be at the second measurement point 120 meters from point 0 with a landslide thickness of approximately 5 meters. The landslide material was soil mixed with sand. The type of slip plane is translational, where the movement of soil and rock masses on the slip plane is flat or has gentle waves. On this track, the slope is steep enough so that the soil mass can slide down.

Following results of data interpretation on the fourth track can be seen in Figure 4.

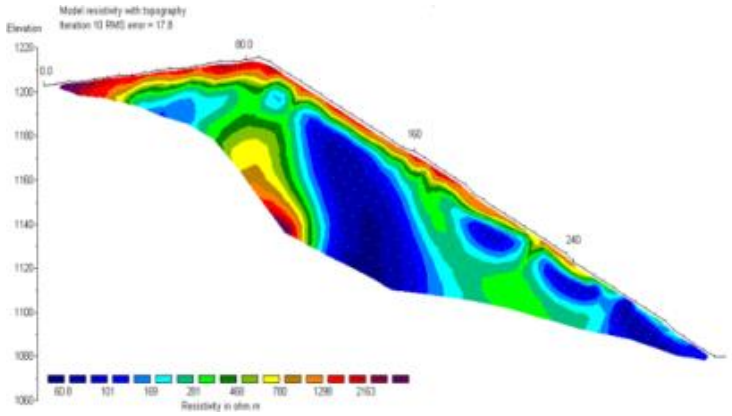

Fig 4. Distribution of resistivity and track depth 4

Based on Figure 4 stretches from coordinates (00'22.491 S, 100'16.880', altitude 1203 masl) to (00'22.514 S, 100'16.738', altitude 1080 masl). The distribution of resistivity anomalies with an initial Damping Factor of 0.25 and a minimum Damping Factor of 0.1. The resistivity value is 60.8 Ωm – 2163 Ωm with an error percentage of 17.8%. Identification of rock types, thickness and depth of subsurface layers along Track 4 was taken at several measurement points, namely 80 meters from point 0 (top point), 120 meters from point 0, 160 meters from point 0, 200 meters from point 0 and 240 meters from point zero.

At the first point, 80 meters from point 0, two rock layers were identified: gneiss and dolomite. Limestone is 34 meters thick and lies 1170-1204 meters above sea level, and dolomite is 10 meters thick and lies 1205-1215 meters below sea level.

At the second point, 120 meters from point 0, three rock layers were identified: clay, limestone, and sand. Clay is at a depth of 1130–1184 meters above sea level and has a thickness of 54 meters; limestone is at a depth of 1185–1189 meters and has a thickness of 4 meters; and sand is at a depth of 1190–1200 meters and has a thickness of 10 meters.

At the third point, 160 meters from point 0, three layers of rock were found: clay, clay, and sand. The clay layer is at a depth of 1110-1139 meters above sea level, with a thickness of 29 meters; clay is at a depth of 1140-1174 meters, with a thickness of 34 meters, and sand is at a depth of 1175-1180 meters, with a thickness of 5 meters.

At the fourth point, 200 meters from point 0, three rock layers were identified: clay, clay, and sand. Clay is at a depth of 1120–1129 meters above sea level and has a thickness of 9 meters, and sand is at a depth of 1150–1155 meters above sea level and has a thickness of 5 meters.

At the fifth point, 240 meters from point 0, three rock layers were identified: a salt layer, a clay layer, and a sand layer. The salt layer is at a depth of 1100-1109 meters and has a thickness of 9 meters; the clay layer is at a depth of 1110-1134 meters and has a thickness of 24 meters, and the sand layer is at a depth of 1135-1140 meters and has a thickness of 15 meters.

The results of data interpretation show that on this route there are several rock layers. At the first measurement point, 80 meters from point 0, it is dominated by dolomite and limestone rocks. At the second measurement point, 120 meters from point 0, it is dominated by clay with a thickness of 54 meters. At this measurement point there is a slip area. At the fifth measurement point, 240 meters from point 0, it is dominated by sandstone, limestone and clay. The presence of very thick clay can affect the presence of rocks beneath it and can trigger landslides. The difference in mechanical properties between hard Limestone and plastic clay can cause deformation or unstable soil movement. The presence of sandstone above the slip surface can also affect overall slope stability. Clay tends to be more susceptible to changes in moisture or pressure, which can cause soil movement. The overlying sandstone can also be a potential zone for friction or deformation, which can increase the risk of landslides. On this route, small scale landslides will occur because this route is a fairly steep hill.

Following results of data interpretation on the fifth track can be seen in Figure 5.

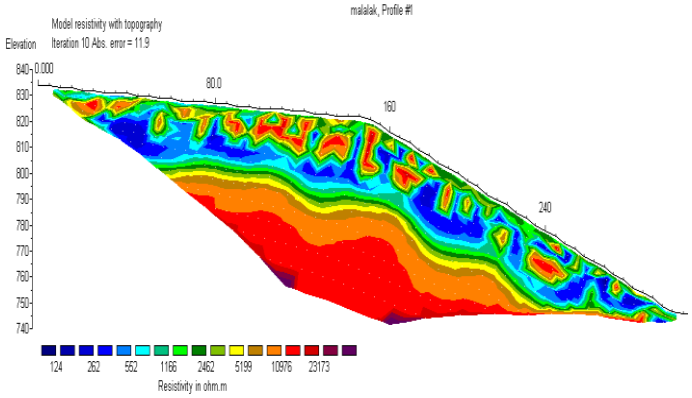

Fig 5. Distribution of resistivity and path depth 5

Based on Figure 5 stretches from coordinates (00'25.496 S, 100'16.357', height 834 masl) to ith (00'25.452 S, 100'16.273', height 746 masl). Landslides have never occurred on this route because there is no slip surface at this location. Shows the distribution of resistivity anomalies with an initial damping factor of 0.2 and a minimum damping factor of 0.03. The resistivity value is 124 Ωm – 23173 Ωm with an error percentage of 11.9%. Identification of rock types, thickness and depth of subsurface layers along Track 4 was taken at several measurement points, namely 80 meters from point 0 (top point), 120 meters from point 0, 160 meters from point 0, 200 meters from point 0 and 240 meters from point zero.

At 80 meters from point 0, four rock layers were discovered: tuff, caracal, sand mixed with lime, and gabbro. Tuff is at a depth of 785-789 meters above sea level, with a thickness of 4 meters, caracal at a depth of 790-799 meters, with a thickness of 9 meters, and sand mixed with lime at a depth of 807-819 meters, with a thickness of 12 meters. Gabbro is at a depth of 820-830 meters, sand mixed with lime at a depth of 820-830 meters, and sand mixed with lime.

At the second point, 120 meters from point 0, four rock layers were identified: tuff, gabbro, sand mixed with lime, and caracal. Tuff is at a depth of 755-779 meters above sea level with a thickness of 24 meters; gabbro is at a depth of 795-799 meters above sea level with a thickness of 5 meters, and sand mixed with lime is at a depth of 800-809 meters above sea level with 9 meters thick. Karakal is at a depth of 810-828 meters above the spring

At the third point, 160 meters from point 0, four rock layers were identified: tuff, gabbro, sand mixed with lime, and caracal. Tuff is at a depth of 745-779 meters above sea

level with a thickness of 34 meters, gabbro is at a depth of 790-799 meters above sea level with a thickness of 9 meters, and sand mixed with lime is at a depth of 800-814 meters above sea level with thickness 14 meters. Karakal is at a depth of 815-820 meters above sea level.

At the fourth point, 200 meters from point 0, four rock layers were identified: tuff, caracal, sand mixed with lime, and gabbro. Tuff is at a depth of 745-754 meters above sea level with a thickness of 9 meters, caracal is at a depth of 755-777 meters above sea level with a thickness of 22 meters, and sand mixed with lime is at a depth of 785-794 meters above sea level with 9 meters thick. Gabbro is at a depth of 795-805 meters above the spring.

At the fifth point, 240 meters from point 0, three rock layers were identified: caracal, sand mixed with lime, and gabbro. Karakal is at a depth of 770-779 meters and 755-759 meters above sea level with a thickness of 4-9 meters. Sand mixed with lime has a depth of 780-784 meters and 760-769 meters above sea level, with a thickness of 9 meters. Gabbro is at a depth of 885-790 meters above sea level with a thickness of 15 meters.

The results of data interpretation show that on this route there are several rock layers. At the first measurement point 80 meters from point 0, it is dominated by Gabbro rock, sand mixed with lime and carakal. Gabbro and Karakal rocks tend to be more resistant to erosion and weathering.

At the second measurement point to the fourth measurement point, 200-120 meters from point 0, it is dominated by carakal rock, sand mixed with lime, gabbro and granite. Very thick granite is interbedded with Karakal rock which is beneath Gabbro rock, and Clay rock. The presence of thick granite rocks under Karakal and Gabbro rocks can influence underground water flow patterns. At the fifth measurement point, 240 meters from point 0, it is dominated by clay rock within the gabbro rock. Clay rocks within gabbro rocks reflect a condition where geological processes such as intrusion or deposition have occurred in the past. There are no landslides on this track, because there are no slip areas on this track. Some types of plants are more likely to grow on the more fertile rocks of Karakal, while others may be better suited to growing on thicker tuff rocks.

Following results of data interpretation on the sixth track can be seen in Figure 6.

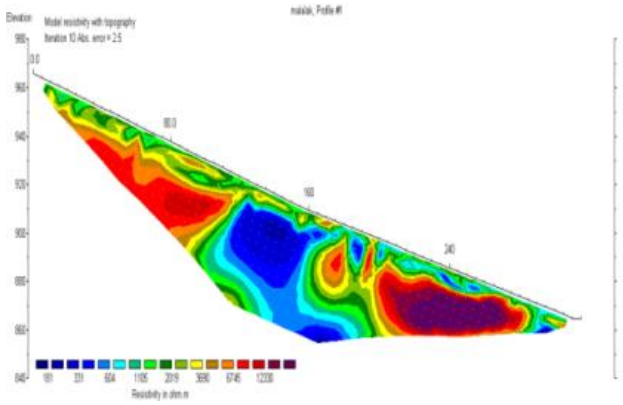

Fig 6. Distribution of resistivity and path depth 5

Based on Figure 6 stretches from coordinates (00'24.618 S, 100'16.740', altitude 966 meters above sea level) to (00'24.576 S, 100'16.596', altitude 865 meters above sea level). There has never been a landslide disaster because, at this location, no-slip surface was formed. Shows the distribution of resistivity anomalies with an initial Damping Factor of 0.25 and a minimum Damping Factor of 0.01. The resistivity value is 181 Ωm – 12330 Ωm with an error percentage of 2.5%. Identification of rock types, thickness and depth of subsurface layers along Route 6 was taken at several measurement points, namely 80 meters from point 0 (top point), 120 meters from point 0, 160 meters from point 0, 200 meters from point 0 and 240 meters from point zero.

At 80 meters from point 0, three rock layers were identified: tuff, caracal, and gabbro. Tuff is at a depth of 902-924 meters and has a thickness of 22 meters, caracal is at a depth of 925-931 meters and has a thickness of 6 meters, and gabbro is at a depth of 932-940 meters and has a thickness of 8 meters.

At the second point, 120 meters from point 0, two rock layers were identified: clayey sand and gabbro. The clayey sand is at a depth of 885-894 meters with a thickness of 19 meters, and the gabbro is at a depth of 985-930 meters and 884-870 meters with a thickness of 14-35 meters above sea level.

At the third point, 160 meters from point 0, two rock layers were found: clayey sand and gabbro. The clayey sand is 890-909 meters and 860-869 meters above sea level, with a thickness of 9-19 meters. Gabbro is at a depth of 910-920 meters and 870-889 meters above sea level, with a thickness of 10-19 meters.

At the fourth point, 200 meters from point 0, two rock layers were identified: tuff and clayey sand. Tuff is at a depth of 860-889 meters above sea level and has a thickness of 29 meters, while clayey sand is at a depth of 890-910 meters above sea level and has a thickness of 20 meters.

At the fifth point, 240 meters from point 0, two rock layers were identified: tuff and clayey sand. Tuff is at a depth of 860-889 meters above sea level and has a thickness of 29 meters, while clayey sand is at a depth of 890-900 meters above sea level and has a thickness of 10 meters.

DISCUSSION

The results of data interpretation show that on this route there are several rock layers. At the first measurement point 80 meters from point 0 it is dominated by Gabbro, carakal and tuff rocks. The tuff rocks are within the Karakal rocks, which are beneath the Gabbro rocks. Tuff rocks are generally softer and more susceptible to weathering compared to Karakal and Gabbro rocks. With tuff rock within the Karakal rock, there could be a reduction in the overall strength of the rock structure which could affect slope stability.

At the second and third measurement points, 160-120 meters from point 0, it is dominated by gabbro rock and clayey sand. At the fourth and fifth measurement points 240-200 meters from point 0, it is dominated by clayey sandstone and tuff. On this track there are no slip areas because the presence of tuff rocks affects plant growth due to its ability to hold water and organic material. The 2-D resistivity cross-section resulting from least-squares inversion with an optimal damping factor shows a 2-D cross-section which shows the existence of a slip plane on track 1 to track 4 with a depth of around 23 meters and a slope of around 43.21°. Comparison of resistivity results makes it possible to determine the level of critical criteria for landslides, where this condition contributes to developing a landslide early warning system using geoelectric methods. The slope of the slope is the main factor in the occurrence of landslides. The steeper the slope, the greater the shear force of the soil under pressure from gravity, which will disrupt the stability of the slope. A slope of 50° produces greater landslide time and volume than a slope of 40°. A slope slope of 50° can produce a greater landslide time and landslide volume because a steep slope produces a greater material pushing force as well(Sapulete dkk., 2019).

CONCLUSION

Based on the interpretation of data that has been carried out starting from track 1 to track 6 using Res2dinv Software with the Least-square Inversion method, Wenner - Schlumberger configuration, the suitable range of damping factors in Malalak Agam District, West Sumatra, namely the initial damping factor (0.2 - 0.25) and the minimum damping factor (0.01 - 0.1) on track 2 At the third measurement point, 160 meters from point 0 is dominated by limestone and sandstone. The existence of Limestone acts as a slip field, and there is Sandstone right above it which causes large-scale landslides from the first to fifth measurement points (160-315 meters from point 0) and on trajectory 3 at this time there is a landslide with a small volume, it is estimated that the avalanche is at the second measurement point 120 meters from point 0 with an avalanche thickness ranging from approximately 5 meters.

REFERENCES

Akmam, A. (2018). Analisis Struktur Batuan Dengan Metoda Inversi Smoothness-Constrained Least-Squares Data Geolistrik Konfigurasi Schlumberger Di Universitas Negeri Padang Kampus Air Tawar. Https://Doi.Org/10.31227/Osf.Io/D82as

Argobi, M. R. (T.T.). Identifikasi Lapisan Batuan Daerah Rawan Longsor Dengan Metode Geolistrik Konfigurasi Wenner-Schlumberger Di Desa Sagalaherang Kaler Kabupaten Subang Jawa Barat.

Binley, A., Hubbard, S. S., Huisman, J. A., Revil, A., Robinson, D. A., Singha, K., & Slater, L. D. (2015). The Emergence Of Hydrogeophysics For Improved Understanding Of Subsurface Processes Over Multiple Scales. Water Resources Research, 51(6), 3837–3866. Https://Doi.Org/10.1002/2015wr017016

Gallardo, L. A., & Meju, M. A. (2011). Structure-Coupled Multiphysics Imaging In Geophysical Sciences. Reviews Of Geophysics, 49(1), 2010rg000330. Https://Doi.Org/10.1029/2010rg000330

Gupta, P. K., Niwas, S., & Gaur, V. K. (1997). Straightforward Inversion Of Vertical Electrical Sounding Data. Geophysics, 62(3), 775–785. Https://Doi.Org/10.1190/1.1444187

Hansen, P. C. (2010). Discrete Inverse Problems: Insight And Algorithms. Society For Industrial And Applied Mathematics.

J. (2013). Effects Of Electrode Spacing And Inversion Techniques On The Efficacy Of 2d Resistivity Imaging To Delineate Subsurface Features. American Journal Of Applied Sciences, 10(1), 64–72. Https://Doi.Org/10.3844/Ajassp.2013.64.72

Jamaluddin, & Umar, E. P. (2018). Identification Of Subsurface Layer With Wenner-Schlumberger Arrays Configuration Geoelectrical Method. Iop Conference Series:

Earth And Environmental Science, 118, 012006. Https://Doi.Org/10.1088/1755-1315/118/1/012006

Lestari, H., Nasri, M., Zulkifli, A., Aswad, S., & Syamsuddin. (2019). Interpretation Of One Dimensional Schlumberger Curve Resistivity Data Using "Least Square" Inversion. Iop Conference Series: Earth And Environmental Science, 279(1), 012042. Https://Doi.Org/10.1088/1755-1315/279/1/012042

Melani, O., Fara, T. A., Anjelika, L., Safitri, D. E., Wibowo, R. C., & Zaelani, A. (2021). Penerapan Metode Inversi Dalam Pendugaan Nilai Resistivitas. Teknika Sains: Jurnal Ilmu Teknik, 6(2), 91–101. Https://Doi.Org/10.24967/Teksis.V6i2.1413

Mulia, I. E., Gusman, A. R., Jakir Hossen, M., & Satake, K. (2018). Adaptive Tsunami Source Inversion Using Optimizations And The Reciprocity Principle. Journal Of Geophysical Research: Solid Earth, 123(12). Https://Doi.Org/10.1029/2018jb016439

Okechukwu, E., & Abanum, B. C. (2020). Lithostratigraphic Characterizationof The Subsurface In Ologbo Community Using Wenner-Schlumberger Electrode Configuration Of Electrical Resistivity Method. International Journal Of Advances In Scientific Research And Engineering, 06(06), 46–56. Https://Doi.Org/10.31695/Ijasre.2020.33830

Olubusola, I., Daniel, A., & Oladimeji, O. (2018). Modeling Of Groundwater Yield Using Gis And Electrical Resistivity Method In A Basement Complex Terrain, Southwestern Nigeria. Journal Of Geography, Environment And Earth Science International, 16(1), 1–17. Https://Doi.Org/10.9734/Jgeesi/2018/42102

Pasa'bi, O. (2021). Pemodelan Dua Dimensi Data Direct Current Resistivity (Dcr) Konfigurasi Wenner-Schlumberger Menggunakan Inversi Least Square.

Permana, R. S., Buana, A. P., Akmam, A., Amir, H., & Putra, A. (2020). Using The Schlumberger Configuration Resistivity Geoelectric Method To Estimate The Rock Structure At Landslide Zone In Malalak Agam. Journal Of Physics: Conference Series, 1481(1), 012034. Https://Doi.Org/10.1088/1742-6596/1481/1/012034

Pimienta, L., Orellana, L. F., & Violay, M. (2019). Variations In Elastic And Electrical Properties Of Crustal Rocks With Varying Degree Of Microfracturation. Journal Of Geophysical Research: Solid Earth, 124(7), 6376–6396. Https://Doi.Org/10.1029/2019jb017339

Rahmani, T. R., Sari, D. P., Akmam, A., Amir, H., & Putra, A. (2020). Using The Schlumberger Configuration Resistivity Geoelectric Method To Analyze The Characteristics Of Slip Surface At Solok. Journal Of Physics: Conference Series, 1481(1), 012030. Https://Doi.Org/10.1088/1742-6596/1481/1/012030

Rolia, E., & Sutjiningsih, D. (2018). Application Of Geoelectric Method For Groundwater Exploration From Surface (A Literature Study). 020018. Https://Doi.Org/10.1063/1.5042874

Sapulete, S. M., Souisa, M., & Jubaedah, S. (2019). Interpretasi Data Resistivitas Untuk Mengidentifikasi Munculnya Longsor Susulan Di Blok V Wayame Ambon. Barekeng: Jurnal Ilmu Matematika Dan Terapan, 13(3), 185–196. Https://Doi.Org/10.30598/Barekengvol13iss3pp185-196ar926

Sari, W. P. (2018). Analisis Struktur Batuan Berdasarkan Data Geolistrik Tahanan Jenis Konfigurasi Schlumberger Dan Konfigurasi Dipole-Dipole Di Kecamatan Malalak Kabupaten Agam. 11(2).

Sheishah, D., Sipos, G., Hegyi, A., Kozák, P., Abdelsamei, E., Tóth, C., Onaca, A., & Páll, D. (2022). Assessing The Structure And Composition Of Artificial Levees Along The Lower Tisza River (Hungary). Geographica Pannonica, 26(3), 258–272. Https://Doi.Org/10.5937/Gp26-39474